# Nonstandard Neutrino Interactions as a Solution to the NO$\nu$A and T2K Discrepancy

Sabya Sachi Chatterjee[1,*] and Antonio Palazzo[2,3,†]

[1] *Institute for Particle Physics Phenomenology, Department of Physics, Durham University, Durham, DH1 3LE, United Kingdom*
[2] *Dipartimento Interateneo di Fisica "Michelangelo Merlin," Via Amendola 173, 70126 Bari, Italy*
[3] *Istituto Nazionale di Fisica Nucleare, Sezione di Bari, Via Orabona 4, 70126 Bari, Italy*

(Received 17 August 2020; accepted 3 December 2020; published 4 February 2021)

The latest data of the two long-baseline accelerator experiments NO$\nu$A and T2K, interpreted in the standard three-flavor scenario, display a discrepancy. A mismatch in the determination of the standard *CP* phase $\delta_{\rm CP}$ extracted by the two experiments is evident in the normal neutrino mass ordering. While NO$\nu$A prefers values close to $\delta_{\rm CP} \sim 0.8\pi$, T2K identifies values of $\delta_{\rm CP} \sim 1.4\pi$. Such two estimates are in disagreement at more than 90% C.L. for 2 degrees of freedom. We show that such a tension can be resolved if one hypothesizes the existence of complex neutral-current nonstandard interactions (NSIs) of the flavor changing type involving the $e-\mu$ or the $e-\tau$ sectors with couplings $|\varepsilon_{e\mu}| \sim |\varepsilon_{e\tau}| \sim 0.2$. Remarkably, in the presence of such NSIs, both experiments point towards the same common value of the standard *CP* phase $\delta_{\rm CP} \sim 3\pi/2$. Our analysis also highlights an intriguing preference for maximal *CP* violation in the nonstandard sector with the NSI *CP* phases having best fit close to $\phi_{e\mu} \sim \phi_{e\tau} \sim 3\pi/2$, hence pointing towards imaginary NSI couplings.

DOI: 10.1103/PhysRevLett.126.051802

*Introduction.*—The two long-baseline (LBL) accelerator experiments NO$\nu$A and T2K have recently released new data at the Neutrino 2020 Conference [1,2]. Intriguingly, the two experiments display a moderate tension preferring values of the standard three-flavor *CP* phase $\delta_{\rm CP}$ which are in disagreement. While this discrepancy may be imputable to a statistical fluctuation or to an unknown systematic error, it may represent an indication of physics beyond the standard model (SM). In particular, one should note that the two experiments are different with respect to their sensitivity to the matter effects, due to the different baselines (810 km for NO$\nu$A and 295 km for T2K). This evokes the fascinating possibility that new physics may be at work in the form of nonstandard neutrino interactions (NSIs).

*Theoretical framework.*—NSIs may constitute the low-energy manifestation of high-energy physics of new heavy states (for a review see Refs. [3–7]) or, they can be related to light mediators [8,9]. As first noted in Ref. [10], NSIs can alter the dynamics [10–12] of the neutrino flavor conversion in matter. The presence of NSIs can have a sizable impact on the interpretation of current LBL data. Notably, in the recent work Ref. [13], it has been evidenced that they may even obscure the correct determination of the neutrino mass ordering (NMO) [14]. The impact of NSIs on present and future new-generation LBL experiments has been widely explored (see for example Refs. [15–38].) The NSIs can be represented by a dimension-six operator [10]

$$\mathcal{L}_{\rm NSI} = -2\sqrt{2}G_F\varepsilon_{\alpha\beta}^{fC}(\bar{\nu_\alpha}\gamma^\mu P_L\nu_\beta)(\bar{f}\gamma_\mu P_C f), \tag{1}$$

where $\alpha, \beta = e, \mu, \tau$ indicate the neutrino flavor, $f = e, u, d$ denote the matter fermions, $P$ represents the projector operator with superscript $C = L, R$ referring to the chirality of the $ff$ current, and $\varepsilon_{\alpha\beta}^{fC}$ are the strengths of the NSIs. The hermiticity of the interaction implies

$$\varepsilon_{\beta\alpha}^{fC} = (\varepsilon_{\alpha\beta}^{fC})^*. \tag{2}$$

For neutrino propagation in the Earth, the relevant combinations are

$$\varepsilon_{\alpha\beta} \equiv \sum_{f=e,u,d} \varepsilon_{\alpha\beta}^{f}\frac{N_f}{N_e} \equiv \sum_{f=e,u,d} (\varepsilon_{\alpha\beta}^{fL} + \varepsilon_{\alpha\beta}^{fR})\frac{N_f}{N_e}, \tag{3}$$

$N_f$ being the number density of the $f$ fermion. For the Earth, we can consider neutral and isoscalar matter, with $N_n \simeq N_p = N_e$, in which case $N_u \simeq N_d \simeq 3N_e$. Therefore,

$$\varepsilon_{\alpha\beta} \simeq \varepsilon_{\alpha\beta}^{e} + 3\varepsilon_{\alpha\beta}^{u} + 3\varepsilon_{\alpha\beta}^{d}. \tag{4}$$

The NSIs alter the effective Hamiltonian of neutrino propagation in matter, which in the flavor basis reads

$$H = U \begin{bmatrix} 0 & 0 & 0 \\ 0 & k_{21} & 0 \\ 0 & 0 & k_{31} \end{bmatrix} U^{\dagger} + V_{\rm CC} \begin{bmatrix} 1+\varepsilon_{ee} & \varepsilon_{e\mu} & \varepsilon_{e\tau} \\ \varepsilon_{e\mu}^{*} & \varepsilon_{\mu\mu} & \varepsilon_{\mu\tau} \\ \varepsilon_{e\tau}^{*} & \varepsilon_{\mu\tau}^{*} & \varepsilon_{\tau\tau} \end{bmatrix}, \quad (5)$$

where $U$ is the Pontecorvo-Maki-Nakagawa-Sakata (PMNS) matrix, which depends on three mixing angles ($\theta_{12}, \theta_{13}, \theta_{23}$) and the $CP$ phase $\delta_{\rm CP}$. The parameters $k_{21} \equiv \Delta m_{21}^2/2E$ and $k_{31} \equiv \Delta m_{31}^2/2E$ represent the solar and atmospheric wave numbers, where $\Delta m_{ij}^2 \equiv m_i^2 - m_j^2$, while $V_{\rm CC}$ is the charged-current matter potential

$$V_{\rm CC} = \sqrt{2} G_F N_e \simeq 7.6 Y_e \times 10^{-14} \left[\frac{\rho}{\rm g/cm^3}\right] \text{eV}, \quad (6)$$

where $Y_e = N_e/(N_p + N_n) \simeq 0.5$ is the relative electron number density in the Earth's crust. It is useful to introduce the dimensionless quantity $v = V_{\rm CC}/k_{31}$, which measures the sensitivity to matter effects. Its absolute value

$$|v| = \left|\frac{V_{\rm CC}}{k_{31}}\right| \simeq 8.8 \times 10^{-2} \left[\frac{E}{\rm GeV}\right], \quad (7)$$

will appear in the expressions of the $\nu_\mu \to \nu_e$ conversion probability. We here emphasize that in T2K (NO$\nu$A) the first oscillation maximum is reached respectively for $E \simeq 0.6$ GeV ($E \simeq 1.6$ GeV). This implies that matter effects are a factor of 3 bigger in NO$\nu$A ($v \simeq 0.14$) than in T2K ($v \simeq 0.05$). This suggests that NO$\nu$A may be sensitive to NSIs to which T2K is basically insensitive, so explaining the apparent disagreement among the two experiments when their results are interpreted in the standard three-flavor scheme.

In the present Letter, we focus on flavor nondiagonal NSIs, that is $\varepsilon_{\alpha\beta}$'s with $\alpha \neq \beta$. We remark that only such flavor-changing NSIs carry out a dependency on a new $CP$ phase, which is a crucial ingredient to resolve the discrepancy between NO$\nu$A and T2K we are considering. More specifically, we consider the couplings $\varepsilon_{e\mu}$ and $\varepsilon_{e\tau}$, which, as will we discuss below, introduce a dependency on their associated $CP$ phase in the appearance $\nu_\mu \to \nu_e$ probability [39]. Let us focus on the conversion probability relevant for the LBL experiments T2K and NO$\nu$A. In the presence of NSIs, the probability can be expressed as the sum of three terms [42],

$$P_{\mu e} \simeq P_0 + P_1 + P_2, \quad (8)$$

which, using a compact notation similar to Ref. [22], take the following forms:

$$P_0 \simeq 4 s_{13}^2 s_{23}^2 f^2, \quad (9)$$

$$P_1 \simeq 8 s_{13} s_{12} c_{12} s_{23} c_{23} \alpha f g \cos(\Delta + \delta_{\rm CP}), \quad (10)$$

$$P_2 \simeq 8 s_{13} s_{23} v |\varepsilon| [a f^2 \cos(\delta_{\rm CP} + \phi) + b f g \cos(\Delta + \delta_{\rm CP} + \phi)], \quad (11)$$

where $\Delta \equiv \Delta m_{31}^2 L/4E$ is the atmospheric oscillating frequency, $L$ is the baseline and $E$ the neutrino energy, and $\alpha \equiv \Delta m_{21}^2/\Delta m_{31}^2$. For brevity, we have used the notation ($s_{ij} \equiv \sin\theta_{ij}$, $c_{ij} \equiv \cos\theta_{ij}$), and following Ref. [43], we have introduced

$$f \equiv \frac{\sin[(1-v)\Delta]}{1-v}, \qquad g \equiv \frac{\sin v\Delta}{v}. \quad (12)$$

In Eq. (11) we have assumed for the NSI coupling the general complex form

$$\varepsilon_{\alpha\beta} = |\varepsilon_{\alpha\beta}| e^{i\phi_{\alpha\beta}}. \quad (13)$$

The expression of $P_2$ is different for $\varepsilon_{e\mu}$ and $\varepsilon_{e\tau}$ and, in Eq. (11) one has to make the replacements

$$a = s_{23}^2, \qquad b = c_{23}^2 \quad \text{if } \varepsilon = |\varepsilon_{e\mu}| e^{i\phi_{e\mu}}, \quad (14)$$

$$a = s_{23} c_{23}, \qquad b = -s_{23} c_{23} \quad \text{if } \varepsilon = |\varepsilon_{e\tau}| e^{i\phi_{e\tau}}. \quad (15)$$

In the expressions given in Eqs. (9)–(11) for $P_0$, $P_1$, and $P_2$, the sign of $\Delta$, $\alpha$, and $v$ is positive (negative) for normal (inverted) ordering NO (IO). We recall that the expressions of the probability provided above hold for neutrinos and that the corresponding formulae for antineutrinos can be derived by flipping in Eqs. (9)–(11) the sign of all the $CP$ phases and of the matter parameter $v$. Finally, we observe that the third term $P_2$ encodes the dependency on the (complex) NSI coupling and it is different from zero only in matter (i.e., if $v \neq 0$). It is generated by the interference of the matter potential $\varepsilon_{e\mu} V_{\rm CC}$ (or $\varepsilon_{e\tau} V_{\rm CC}$) with the atmospheric wave number $k_{31}$ (see the discussion in Ref. [15]) [44].

*Data used in the analysis.*—We extracted the datasets of NO$\nu$A and T2K from the latest data released in Refs. [1,2]. We fully incorporate both the disappearance and appearance channels in both experiments. In our analysis we use the software GLoBES [46,47] and its additional public tool [48], which can implement NSIs. In our analysis we have marginalized over $\theta_{13}$ with 3.4% 1 sigma prior with central value $\sin^2\theta_{13} = 0.0219$ as determined by Daya Bay [49]. We have fixed the solar parameters $\Delta m_{21}^2$ and $\theta_{12}$ at their best fit values estimated in the recent global analysis [50].

*Numerical results.*—Figure 1 reports the results of the analysis of the combination of T2K and NO$\nu$A for NO (left panels) and IO (right panels). The upper (lower) panels refer to $\varepsilon_{e\mu}$ ($\varepsilon_{e\tau}$) taken one at a time. Each panel displays the allowed regions in the plane spanned by the relevant NSI coupling and the standard $CP$ phase $\delta_{\rm CP}$. The nonstandard $CP$ phases, the mixing angles $\theta_{23}$ and $\theta_{13}$, and the squared-mass $\Delta m_{31}^2$ are marginalized away. We display the allowed

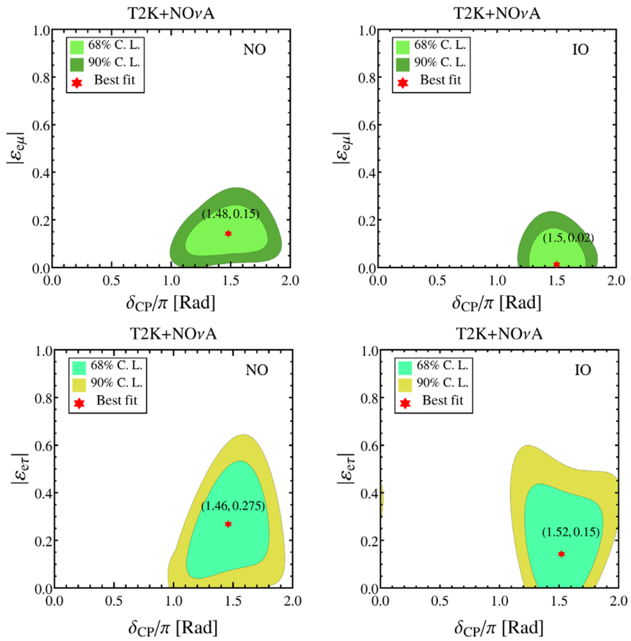


FIG. 1. Allowed regions determined by the combination of T2K and NOνA for NO (left panels) and IO (right panels). The upper (lower) panels refer to $\varepsilon_{e\mu}(\varepsilon_{e\tau})$ taken one at a time. In the upper (lower) panels the NSI *CP* phase $\phi_{e\mu}$ ($\phi_{e\tau}$) has been marginalized. In all panels the atmospheric parameters $\Delta m^2_{31}$ and $\theta_{23}$ have been marginalized. The contours are drawn at the 68% and 90% confidence level for 2 DOF.

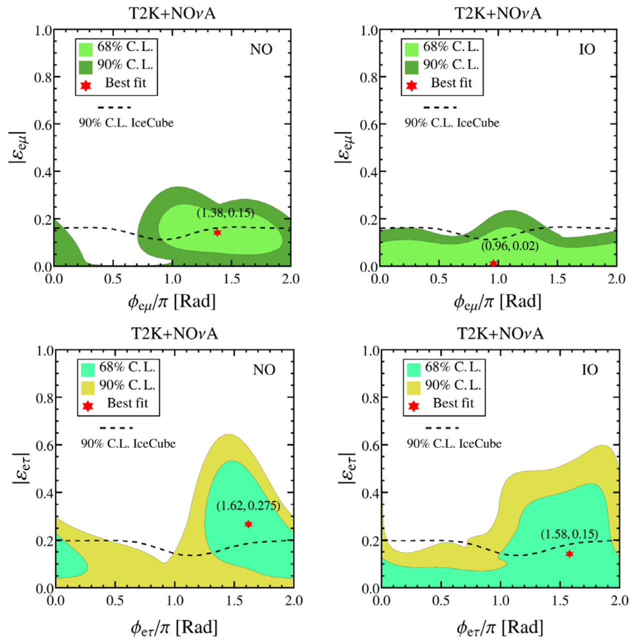


FIG. 2. Allowed regions determined by the combination of T2K and NOνA for NO (left panels) and IO (right panels). The upper (lower) panels refer to $\varepsilon_{e\mu}(\varepsilon_{e\tau})$ taken one at a time. In all panels the standard *CP* phase $\delta_{CP}$ has been marginalized in addition to the atmospheric parameters $\Delta m^2_{31}$ and $\theta_{23}$. The contours are drawn at the 68% and 90% confidence level for 2 DOF. The dashed curves represent the upper bounds (90% C.L., 2 DOF) derived from the preliminary analysis of the IceCube data [51].

regions at the 68% and 90% confidence level for 2 DOF, and denote with a star the best fit point. From the left upper panel we can appreciate that in NO there is a $\sim 2.1\sigma$ ($\Delta\chi^2 = 4.50$) preference for a nonzero value of the coupling $|\varepsilon_{e\mu}|$, with best fit $|\varepsilon_{e\mu}| = 0.15$. In the right upper panel we see that in IO the preference for NSIs is negligible. The lower panels depict the situation for the coupling $|\varepsilon_{e\tau}|$. In NO there is a preference at the $1.9\sigma$ ($\Delta\chi^2 = 3.75$) with best fit $|\varepsilon_{e\tau}| = 0.27$, while in IO the preference is only at the $1.0\sigma$ with best fit $|\varepsilon_{e\tau}| = 0.15$. It is interesting to note how in all four cases the preferred value for the *CP* phase $\delta_{CP}$ is close to $3\pi/2$. We will come back later on this important point.

Figure 2 shows the results of the analysis of the combination of T2K and NOνA similar to Fig. 1. In this case, however, each panel displays the allowed regions in the plane spanned by the relevant NSI coupling ($|\varepsilon_{e\mu}|$ or $|\varepsilon_{e\tau}|$) and the corresponding *CP* phase ($\phi_{e\mu}$ or $\phi_{e\tau}$). The standard *CP* phase $\delta_{CP}$, the mixing angles $\theta_{23}$ and $\theta_{13}$, and the squared mass $\Delta m^2_{31}$ are marginalized away. It is intriguing to note how in the NO case the preferred value for both the new *CP* phases $\phi_{e\mu}$ and $\phi_{e\tau}$ is close to $3\pi/2$, so indicating purely imaginary NSIs, i.e., maximal *CP* violation also in the NSI sector. In Table I we report the best fit values of the NSI couplings together with the *CP* phases and the value of $\Delta\chi^2 = \chi^2_{SM} - \chi^2_{SM+NSI}$ for a fixed choice of the NMO.

In Fig. 2, we superimpose the upper bounds coming from the preliminary analysis of IceCube data [51], which are the most stringent ones in the literature on the relevant couplings. These bounds are not incompatible with the indication we find. Rather, they select the lower values of the couplings favored by T2K and NOνA. Interestingly, IceCube finds $|\varepsilon_{e\mu}| = 0.07$ as the best fit point with a preference of 1 sigma level with respect to the SM case (see slides 20 and 33 in Ref. [51]). Also, the best fit we find for the *CP* phase $\phi_{e\mu} \sim 3\pi/2$ is compatible with that found by IceCube. Although we cannot quantitatively combine our results with those of IceCube, we can estimate that $|\varepsilon_{e\mu}| \sim 0.1$ is expected to come as the best fit from such a combination with a significance around the 2 sigma confidence level.

TABLE I. Best fit values and $\Delta\chi^2 = \chi^2_{SM} - \chi^2_{SM+NSI}$ for the two choices of the NMO.

| NMO | NSI | $\lvert\varepsilon_{\alpha\beta}\rvert$ | $\phi_{\alpha\beta}/\pi$ | $\delta_{CP}/\pi$ | $\Delta\chi^2$ |
|---|---|---|---|---|---|
| NO | $\varepsilon_{e\mu}$ | 0.15 | 1.38 | 1.48 | 4.50 |
| | $\varepsilon_{e\tau}$ | 0.27 | 1.62 | 1.46 | 3.75 |
| IO | $\varepsilon_{e\mu}$ | 0.02 | 0.96 | 1.50 | 0.07 |
| | $\varepsilon_{e\tau}$ | 0.15 | 1.58 | 1.52 | 1.01 |

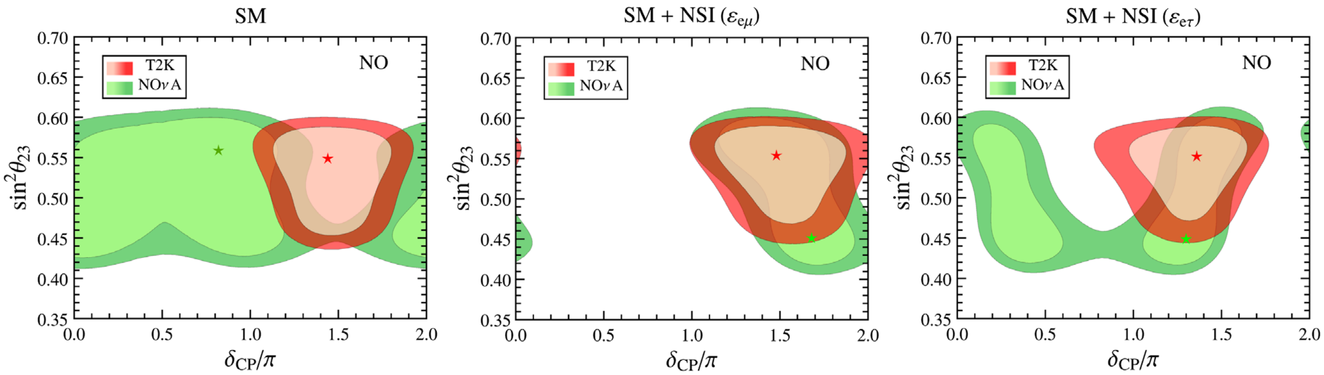


FIG. 3. Allowed regions determined separately by T2K and NO$\nu$A for NO in the SM case (left panel) and with NSI in the $e-\mu$ sector (middle panel) and in the $e-\tau$ sector (right panel). In the middle panel we have taken the NSI parameters at their best fit values of T2K + NO$\nu$A ($|\varepsilon_{e\mu}| = 0.15$, $\phi_{e\mu} = 1.38\pi$). Similarly, in the right panel we have taken $|\varepsilon_{e\tau}| = 0.275$, $\phi_{e\tau} = 1.62\pi$. The contours are drawn at the 68% and 90% C.L. for 2 DOF The comparison of the middle and right panels with the left one clearly evidences the reduction of the tension between the two experiments in the presence of NSI of both types.

In order to understand how the preference for a nonzero NSI coupling arises, it is useful to look to what happens separately to NO$\nu$A and T2K. For this purpose, in Fig. 3 we display the allowed regions in the plane spanned by the standard *CP* phase $\delta_{CP}$ and the atmospheric mixing angle $\theta_{23}$ in the NO case. The left panel refers to the SM case, while the middle and right panels concern the SM + NSI scenario with NSIs in the $e-\mu$ and $e-\tau$ sectors respectively. In the middle and right panels we have taken the NSI parameters at their best fit values of the combined analysis of NO$\nu$A and T2K. More specifically, $|\varepsilon_{e\mu}| = 0.15, \phi_{e\mu} = 1.38\pi$ (middle panel) and $|\varepsilon_{e\tau}| = 0.275, \phi_{e\tau} = 1.62\pi$ (right panel). The contours are drawn at the 68% and 90% C.L. for 2 DOF. In the SM case a clear mismatch in the determination of the *CP* phase $\delta_{CP}$ among the two experiments is evident. While NO$\nu$A prefers values close to $\delta_{CP} \sim 0.8\pi$, T2K identifies a value of $\delta_{CP} \sim 1.4\pi$. Such two estimates, which have a difference of phase of about $\pi/2$, are in disagreement at more than 90% C.L. for 2 DOF. The reduction of the tension between the two experiments obtained in the presence of NSI is evident both in the middle and right panels where the best fit values of $\delta_{CP}$ are very close to the common value $\delta_{CP} \sim 3\pi/2$. We see that the value of $\delta_{CP}$ preferred by T2K is basically unchanged in the presence of NSIs as this experiment has a reduced sensitivity to matter effects. As a consequence the value of $\delta_{CP}^{T2K} \sim 3\pi/2$ identified by T2K can be considered a faithful estimate of its true value both in the SM and in the SM + NSI scenarios. In contrast, NO$\nu$A, due to the enhanced sensitivity to matter effects, if NSIs are not taken into account (left panel), identifies a fake value of $\delta_{CP}^{NO\nu A} \sim 0.8\pi$. In NO$\nu$A, the preference for the true value of $\delta_{CP} \sim 3\pi/2$ is restored once the NSIs are taken into account (middle and right panels). Therefore, it seems that NSIs offer a very simple and elegant way to solve the discrepancy among the two experiments. We also note that the allowed regions for NO$\nu$A are qualitatively different in the $e-\mu$ and $e-\tau$ NSI cases. In fact, in the first case there is a single allowed region while in the second case there are two degenerate lobes. This different behavior can be traced to the fact that the transition probabilities are different in the two cases. More specifically, the sign in front of the coefficient $b$ of $P_2$ in Eq. (11) [see Eqs. (14) and (15)] is opposite in the two scenarios.

For completeness, in the Supplemental Material [52] (which includes Refs. [53–55]), we provide two additional figures. First, we provide a figure analogous to Fig. 3 but referring to the IO case. This plot clarifies why (as shown in Figs. 1 and 2 and also in Table I), in the IO case there is basically no preference for nonzero NSIs. Second, we provide the one-dimensional projections on the standard oscillation parameters $\delta_{CP}$, $\theta_{23}$, and $|\Delta m^2_{31}|$ from the combination of NO$\nu$A and T2K, with and without NSIs.

*Conclusions.*—In this Letter we have investigated the impact of NSIs on the tension recently emerged in the latest T2K and NO$\nu$A data. Our main result is that such a tension can be resolved by nonstandard interactions (NSIs) of the flavor changing type involving the $e$-$\mu$ and $e$-$\tau$ flavors. We underline that, apart from the LBL accelerator data, it would be very important to complement our study considering the atmospheric neutrino data. To this regard, we mention the recent IceCube DeepCore analysis [51], which starts to probe values of the NSI couplings below ~0.2, close but not incompatible to those relevant to the present analysis. We also hope that SuperKamiokande may provide an updated analysis of the atmospheric data in the presence of NSI, which is currently unfeasible from outside the collaboration.

Our results point towards relatively large effective NSI couplings of the order of ten percent. Taking into account Eq. (4), these may correspond to couplings of a few percent at the level of the fundamental constituents ($u$ and $d$ quarks and electrons). A major challenge in generating such observable NSIs in any UV-complete model is that there are stringent bounds arising from charged-lepton flavor violation. In fact, when the new physics responsible for the generation of the neutrino NSIs is due to mediators heavier than the electroweak symmetry-breaking scale, one expects also that the charged leptons are involved as components of the doublet of SU(2). One possible way to circumvent this problem is to increase the complexity of the model. At the tree level, one can consider NSIs generated in models endowed with dimension-8 operators, which typically require the introduction of two mediators [56]. Another possibility, remaining in the framework of heavy-mediators induced NSIs, is to consider NSIs which arise in radiative neutrino mass models (see for example the recent studies [57–59]). A third possibility is to abandon altogether the heavy-mediator paradigm and consider NSIs induced by light mediators (see for example Refs. [8,9]).

In this Letter we have focused on the current data provided by NO$\nu$A and T2K. Needless to say, it would be interesting to consider the sensitivity to NSIs of the future LBL experiments. In particular, we foresee that a careful comparison of T2HK and DUNE should be very informative. On the one hand T2HK, with its short 295 km baseline, should be able to determine the standard parameters almost independently of NSIs. On the other hand, DUNE with its 1300 km baseline should manifest striking effects induced by NSIs and allow their identification. Of course, the determination of the NMO is expected to become more challenging in the presence of new physics. To this respect we underline the importance of experiments like JUNO which are insensitive to (both standard and nonstandard) matter effects and will allow us to identify the NMO (and other standard oscillation parameters) independently of hypothetical NSIs. Finally, we note that independent measurements of the NSI couplings relevant for NO$\nu$A and T2K may also come in the future from experiments that probe the coherent elastic neutrino nucleus scattering.

A. P. acknowledges partial support by the research Grant No. 2017W4HA7S “NAT-NET: Neutrino and Astroparticle Theory Network” under the program PRIN 2017 funded by the Italian Ministero dell’Istruzione, dell’Università e della Ricerca (MIUR), and by the research project *TAsP* funded by the Instituto Nazionale di Fisica Nucleare (INFN).

*Note added.*—Recently, Ref. [55] appeared discussing a similar scenario.

[*]sabya.s.chatterjee@durham.ac.uk
[†]palazzo@ba.infn.it

[1] A. Himmel, *Neutrino 2020, 22 Jun 2020 -2 Jul 2020, Virtual Meeting* (2020), https://doi.org/10.5281/zenodo.4142045.
[2] P. Dunne, *Neutrino 2020, 22 Jun 2020 -2 Jul 2020, Virtual Meeting* (2020), https://doi.org/10.5281/zenodo.4154355.
[3] Y. Farzan and M. Tortola, Front. Phys. **6**, 10 (2018).
[4] C. Biggio, M. Blennow, and E. Fernandez-Martinez, J. High Energy Phys. 08 (2009) 090.
[5] T. Ohlsson, Rep. Prog. Phys. **76**, 044201 (2013).
[6] O. G. Miranda and H. Nunokawa, New J. Phys. **17**, 095002 (2015).
[7] P. S. B. Dev *et al.*, SciPost Phys. Proc. **2**, 001 (2019).
[8] Y. Farzan, Phys. Lett. B **748**, 311 (2015).
[9] Y. Farzan and I. M. Shoemaker, J. High Energy Phys. 07 (2016) 033.
[10] L. Wolfenstein, Phys. Rev. D **17**, 2369 (1978).
[11] S. Mikheev and A. Y. Smirnov, Sov. J. Nucl. Phys. **42**, 913 (1985).
[12] S. Mikheev and A. Y. Smirnov, Nuovo Cimento C **9**, 17 (1986).
[13] F. Capozzi, S. S. Chatterjee, and A. Palazzo, Phys. Rev. Lett. **124**, 111801 (2020).
[14] In the three-flavor scheme there are three mass eigenstates $\nu_i$ with masses $m_i$ ($i = 1, 2, 3$), three mixing angles $\theta_{12}$, $\theta_{13}$, $\theta_{13}$, and one $CP$ phase $\delta_{\rm CP}$. The mass ordering is defined to be normal (inverted) if $m_3 > m_{1,2}$ ($m_3 < m_{1,2}$). We will abbreviate normal (inverted) ordering as NO (IO).
[15] A. Friedland and I. M. Shoemaker, arXiv:1207.6642.
[16] J. A. B. Coelho, T. Kafka, W. A. Mann, J. Schneps, and O. Altinok, Phys. Rev. D **86**, 113015 (2012).
[17] I. Girardi, D. Meloni, and S. T. Petcov, Nucl. Phys. **B886**, 31 (2014).
[18] Z. Rahman, A. Dasgupta, and R. Adhikari, J. Phys. G **42**, 065001 (2015).
[19] P. Coloma, J. High Energy Phys. 03 (2016) 016.
[20] A. de Gouvêa and K. J. Kelly, Nucl. Phys. **B908**, 318 (2016).
[21] S. K. Agarwalla, S. S. Chatterjee, and A. Palazzo, Phys. Lett. B **762**, 64 (2016).
[22] J. Liao, D. Marfatia, and K. Whisnant, Phys. Rev. D **93**, 093016 (2016).
[23] D. V. Forero and P. Huber, Phys. Rev. Lett. **117**, 031801 (2016).
[24] K. Huitu, T. J. Kärkkäinen, J. Maalampi, and S. Vihonen, Phys. Rev. D **93**, 053016 (2016).
[25] P. Bakhti and Y. Farzan, J. High Energy Phys. 07 (2016) 109.
[26] M. Masud and P. Mehta, Phys. Rev. D **94**, 013014 (2016).
[27] C. Soumya and R. Mohanta, Phys. Rev. D **94**, 053008 (2016).
[28] M. Masud and P. Mehta, Phys. Rev. D **94**, 053007 (2016).
[29] A. de Gouvêa and K. J. Kelly, arXiv:1605.09376.
[30] S. Fukasawa, M. Ghosh, and O. Yasuda, Phys. Rev. D **95**, 055005 (2017).
[31] J. Liao, D. Marfatia, and K. Whisnant, J. High Energy Phys. 01 (2017) 071.
[32] J. Liao, D. Marfatia, and K. Whisnant, Phys. Lett. B **767**, 350 (2017).
[33] M. Blennow, S. Choubey, T. Ohlsson, D. Pramanik, and S. K. Raut, J. High Energy Phys. 08 (2016) 090.
[34] K. N. Deepthi, S. Goswami, and N. Nath, Nucl. Phys. **B936**, 91 (2018).
[35] L. J. Flores, E. A. Garces, and O. G. Miranda, Phys. Rev. D **98**, 035030 (2018).
[36] J. M. Hyde, Nucl. Phys. **B949**, 114804 (2019).

[37] M. Masud, S. Roy, and P. Mehta, Phys. Rev. D **99**, 115032 (2019).

[38] I. Esteban, M. Gonzalez-Garcia, and M. Maltoni, J. High Energy Phys. 06 (2019) 055.

[39] The $\nu_\mu \to \nu_\mu$ disappearance channel is sensitive to the $\mu - \tau$ NSIs but this can be safely ignored because of the very strong upper bound put by the atmospheric neutrinos $|\varepsilon_{\mu\tau}| < 8.0 \times 10^{-3}$ [40] (see also Ref. [41]).

[40] M. G. Aartsen *et al.* (IceCube Collaboration), Phys. Rev. D **97**, 072009 (2018).

[41] G. Mitsuka *et al.* (Super-Kamiokande Collaboration), Phys. Rev. D **84**, 113008 (2011).

[42] T. Kikuchi, H. Minakata, and S. Uchinami, J. High Energy Phys. 03 (2009) 114.

[43] V. Barger, D. Marfatia, and K. Whisnant, Phys. Rev. D **65**, 073023 (2002).

[44] Interestingly, an analogous splitting $P_{\mu e} \simeq P_0 + P_1 + P_2$ of the transition probability is valid in the presence of oscillations driven by a sterile neutrino [45]. In that case, however, the term $P_2$ emerges due to the interference between the amplitude driven by the atmospheric mass difference and that by the mass difference corresponding to the sterile neutrino, instead of the interference with the term originated from the matter potential.

[45] N. Klop and A. Palazzo, Phys. Rev. D **91**, 073017 (2015).

[46] P. Huber, M. Lindner, and W. Winter, Comput. Phys. Commun. **167**, 195 (2005).

[47] P. Huber, J. Kopp, M. Lindner, M. Rolinec, and W. Winter, Comput. Phys. Commun. **177**, 432 (2007).

[48] J. Kopp, https://www.mpi-hd.mpg.de/personalhomes/globes/tools/snu-1.0.pdf (2010).

[49] D. Adey *et al.* (Daya Bay Collaboration), Phys. Rev. Lett. **121**, 241805 (2018).

[50] F. Capozzi, E. Di Valentino, E. Lisi, A. Marrone, A. Melchiorri, and A. Palazzo, Phys. Rev. D **95**, 096014 (2017); **101**, 116013(A) (2020).

[51] T. Ehrhardt, *4th Uppsala workshop on Particle Physics with Neutrino Telescopes* (2019), https://indico.uu.se/event/600/contributions/1024/attachments/1025/1394/IceCube_NSI_Search_PPNT19.pdf.

[52] See Supplemental Material at http://link.aps.org/supplemental/10.1103/PhysRevLett.126.051802 for two additional figures. The first one is analogous to Fig. 3 but refers to the IO case. The second one provides the one-dimensional constraints on the standard oscillation parameters obtained from the combination of NO$\nu$A and T2K data, with and without NSIs.

[53] K. J. Kelly, P. A. Machado, S. J. Parke, Y. F. Perez Gonzalez, and R. Zukanovich-Funchal, arXiv:2007.08526.

[54] I. Esteban, M. Gonzalez-Garcia, M. Maltoni, T. Schwetz, and A. Zhou, J. High Energy Phys. 09 (2020) 178.

[55] P. B. Denton, J. Gehrlein, and R. Pestes, preceding Letter, Phys. Rev. Lett. **126**, 051801 (2021).

[56] M. B. Gavela, D. Hernandez, T. Ota, and W. Winter, Phys. Rev. D **79**, 013007 (2009).

[57] K. Babu, P. B. Dev, S. Jana, and A. Thapa, J. High Energy Phys. 03 (2020) 006.

[58] D. V. Forero and W.-C. Huang, J. High Energy Phys. 03 (2017) 018.

[59] U. K. Dey, N. Nath, and S. Sadhukhan, Phys. Rev. D **98**, 055004 (2018).